# Scientific Computing Exercise Set 1

Qinghe Gao (12589896) & Jacobus Dijkman (12864765)

## I. Introduction

MODELLING and simulation have proven to be essential for understanding a great number of complex systems [1]. Two equations that seem to come up in various disciplines are the wave equation and the diffusion equation. The wave equation describes a wide range of phenomena, such as the behaviour of light, sound or water. Likewise, the diffusion equation describes a wide range of phenomenon, ranging from the spread of heat in a medium to the distribution of wealth in an economy [2]. To better understand the various systems which are governed by these equations, a mathematical description of the dynamics of these equations is key. However, due to the inherent complexity of these systems, analytical solutions are often beyond grasp. For these kinds of systems numerical schemes have to be resorted. This report will discuss various numerical schemes for the one dimensional wave equation and the diffusion equation. The theory behind these numerical schemes will be discussed first, after which an analysis will be presented of the different methods discussed in this report.

## II. Theory

### A. The One Dimensional Wave Equation

The mathematical expression for the one dimensional wave equation is shown in equation 1:

$$\frac{\partial^2 \Psi}{\partial t^2} = c^2 \frac{\partial^2 \Psi}{\partial x^2} \tag{1}$$

To derive an numerical expression for the dynamics of this equation, Taylor expansions can be used to find expressions of $\Psi(x + \Delta x)$, $\Psi(x - \Delta x)$, $\Psi(t + \Delta t)$ and $\Psi(t - \Delta t)$. As a first step, the expansions in $x$ are shown in the equations below:

$$\Psi(x+\Delta x) = \Psi(x) + \Delta x \frac{\partial \Psi}{\partial x} + \frac{(\Delta x)^2}{2!} \frac{\partial^2 \Psi}{\partial x^2} + o(x^3) \tag{2}$$

$$\Psi(x-\Delta x) = \Psi(x) - \Delta x \frac{\partial \Psi}{\partial x} + \frac{(\Delta x)^2}{2!} \frac{\partial^2 \Psi}{\partial x^2} + o(x^3) \tag{3}$$

Adding these equations together gives:

$$\frac{\partial^2 \Psi}{\partial x^2} = \frac{\Psi(x + \Delta x) + \Psi(x - \Delta x) - 2\Psi(x)}{(\Delta x)^2} \tag{4}$$

In the same manner, we can add the Taylor expansions in time together, as shown in equation 4 below.

$$\frac{\partial^2 \Psi}{\partial t^2} = \frac{\Psi(t + \Delta t) + \Psi(t - \Delta t) - 2\Psi(t)}{(\Delta t)^2} \tag{5}$$

Substituting equation 4 and 5 into equation 1, we find at discretization of the wave equation (6)

$$\frac{{\Psi_i}^{k+1} + {\Psi_i}^{k-1} - 2{\Psi_i}^{k}}{(\Delta t)^2} = \frac{{\Psi_{i+1}}^{k} + {\Psi_{i-1}}^{k} - 2{\Psi_i}^{k}}{(\Delta x)^2} \tag{6}$$

This expression can be rewritten to arrive at the numerical solution for the time development of the one dimensional wave equation (7).

$${\Psi_i}^{k+1} = 2{\Psi_i}^{k} - {\Psi_i}^{k-1} + \frac{c^2(\Delta t)^2 {\Psi_{i+1}}^{k} + {\Psi_{i-1}}^{k} - 2{\Psi_i}^{k}}{(\Delta x)^2} \tag{7}$$

In equation 7 above, $i$ represents $x \in (1\delta x \ldots N\delta x)$ with $N$ as the number of $x$ intervals. $k$ represents time steps $\delta t$. The exact values for $\delta x$ and $\delta t$ are discussed in the Methods section.

### B. The Time Dependent Diffusion Equation

The two dimensional diffusion equation can be described equation 8:

$$\frac{\partial c}{\partial t} = D \bigtriangledown^2 c \tag{8}$$

In this equation, $D$ represents the diffusion coefficient. $\bigtriangledown^2 c$ is the Jacobian of the concentration:

$$\bigtriangledown^2 c = \frac{\partial^2 c}{\partial x^2} + \frac{\partial^2 c}{\partial y^2} \tag{9}$$

To first define the system which we want to describe numerically, the simplest situation has been taken as example in this report. As shown in figure 1, the boundary and initial condition can be described by equation 10.

$$\begin{cases} c(x, y = 1; t) = 1, c(x, y = 0; t) = 0 \\ c(x = 0, y; t) = c(x = 1, y; t) \\ c(x, y; t = 0) = 0, 0 \leq x \leq 1, 0 \leq y < 1. \end{cases} \quad (10)$$

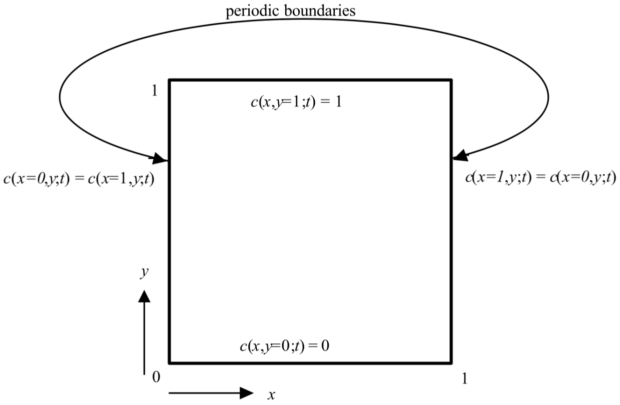

Fig. 1: The computational domain and boundary conditions.

Since this system is symmetrical in x direction, the one dimensional analytical solution depends on y, as shown in equation 11.

$$c(x, t) = \sum_{i=0}^{\infty} \text{erfc}\left(\frac{1 - x + 2i}{2\sqrt{Dt}}\right) - \text{erfc}\left(\frac{1 + x + 2i}{2\sqrt{Dt}}\right) \quad (11)$$

For multiply dimensions and more complex systems, an analytical solution quickly becomes impossible. In these cases, a numerical scheme is needed. In order to do derive this, the domain needs to be discretized. The $x$-axis and $y$-axis of the domain need to be divided in $N$ discrete intervals with $\delta x = \delta y = 1/N$. Then $x = i\delta x$, $y = j\delta x$, where $i, j \in 1 \ldots N$. Additionally, the time progression can be divided into intervals $\delta t$, such that $t = k\delta t$ with $k \in N$.

Similar to the Taylor expansions used for the numerical solution of the one-dimensional wave equation (equations 2 and 3), Taylor expansions of the diffusion equation in $x$ and $y$ direction can be used to find the the numerical expression for the time dependent diffusion equation:

$$\frac{c_{i,j}^{k+1} - c_{i,j}^{k}}{\Delta t} = \frac{D}{(\Delta x)^2} Z \quad (12)$$

with

$$Z = ({c_{i+1,j}}^k + {c_{i-1,j}}^k + {c_{i,j+1}}^k + {c_{i,j-1}}^k - 4{c_{i,j}}^k) \quad (13)$$

From this an explicit scheme for the time development of the concentration can be derived, as shown in equation 14.

$${c_{i,j}}^{k+1} = {c_{i,j}}^k + \frac{D\Delta t}{(\Delta x)^2} Z \quad (14)$$

In order to make this system stable, the following constraint must hold:

$$\frac{4\delta t D}{\delta x^2} \leq 1 \quad (15)$$

Since periodic boundary conditions were used in the model, the equation to use at the boundaries is different. Since the neighbouring lattice points at the left side of the grid are equal to the lattice points at the right side of the grid, the neighbours of the points at both the right side and at the left side of the grid are $(x = 2\delta x, y, t)$ and $(x = (N-1)\delta x, y, t)$. For these points, Z in equation 14 changes to equation 16 below.

$$Z = ({c_{2,j}}^k + {c_{N-1,j}}^k + {c_{i,j+1}}^k + {c_{i,j-1}}^k - 4{c_{i,j}}^k) \quad (16)$$

### *C. The Time Independent Diffusion Equation*

If we are only interested in the equilibrium state of the system, we can use the time independent diffusion equation (equation 17), also called the Laplace equation. To arrive at this equation, we use the fact that at equilibrium, $\frac{\partial c}{\partial t} = 0$ and substitute this equality into the analytical expression of the time dependent diffusion equation (equation 8) to arrive at the expression in equation 17.

$$\nabla^2 c = 0 \quad (17)$$

For the numerical expression of the Laplace equation, we insert the equality $\frac{\partial c}{\partial t} = 0$ into the the numerical expression that we derived for the time dependent diffusion equation (equation 12). This gives $Z = 0$ and from this we find the following set of finite difference equations:

$$c_{i,j} = \frac{1}{4}(c_{i+1,j} + c_{i-1,j} + c_{i,j+1} + c_{i,j-1}) \quad (18)$$

This set of equations can be solved through various methods. One category of methods to solve the equation is iterative methods, which we will focus on in this report. The next section will discuss the three iterative methods used in this report.

*1) The Jacobi Iteration:* The Jacobi iteration directly calculates the concentration at every iteration using equation 18, as shown in equation 19.

$$c_{i,j}^{k+1} = \frac{1}{4}\left(c_{i+1,j}^{k} + c_{i-1,j}^{k} + c_{i,j+1}^{k} + c_{i,j-1}^{k}\right) \tag{19}$$

The iteration is stopped when the maximum change in concentration after an iteration ($\delta$) is smaller than a certain value $\epsilon$ (equation 20).

$$\delta \equiv \max_{i,j}\left|c_{i,j}^{k+1} - c_{i,j}^{k}\right| < \epsilon \tag{20}$$

*2) The Gauss-Seidel Iteration:* The Gauss-Seidel iteration method is similar to the Jacobi method. However, the Gauss-Seidel method uses newly calculated values for the concentration in the same iteration as they have been calculated (equation 21). The stopping condition is the same as for the Jacobi method (equation 20).

$$c_{i,j}^{k+1} = \frac{1}{4}\left(c_{i+1,j}^{k} + c_{i-1,j}^{k+1} + c_{i,j+1}^{k} + c_{i,j-1}^{k+1}\right) \tag{21}$$

*3) Successive Over Relaxation:* The Successive Over Relaxation method improves on the Gauss-Seidel method by introducing a relaxation term $\omega$ in the iteration equation:

$$c_{i,j}^{k+1} = \frac{\omega}{4}\left(c_{i+1,j}^{k} + c_{i-1,j}^{k+1} + c_{i,j+1}^{k} + c_{i,j-1}^{k+1}\right) + (1-\omega)c_{i,j}^{k} \tag{22}$$

The added term $(1-\omega)c_{i,j}^{k}$ causes under-relaxation when $\omega < 1$ and causes over-relaxation if $1 < \omega < 2$. This allows the method to be fine tuned for the best value of $\omega$ for a certain problem.

## III. Methods

### A. One Dimensional Wave Equation

To analyse the numerical solution for the one dimensional wave equation, three string systems were analysed with the following initial conditions:
-$\Psi(x,t=0) = \sin(2\pi x)$
-$\Psi(x,t=0) = \sin(5\pi x)$
-$\Psi(x,t=0) = \sin(5\pi x)$ if $1/5 < x < 2/5$, else $\Psi = 0$.

The boundary conditions of the system are $\Psi(x = 0, t) = 0$, $\Psi(x = L, t) = 0$ and $\Psi(x, t = 0) = f(x)$, with $L$ as the length of the domain and $L = 1$. We assume that at $t = 0$ the string is at rest such that $\Psi'(x, t = 0) = 0$. The axis of the domain were divided into $N = 1000$ intervals, such that $\Delta x = L/N$ in equation 7 becomes $\Delta x = 1/1000$. The values that were used for $c$ and $\Delta t$ in equation 7 were $c = 1$, $\Delta t = 0.001$.

### B. The Time Dependent Diffusion Equation

For the system that was used as discussed in the Theory section of this report (Fig. 1), the initial concentration at every point in space was set at 0 (equation 23).

$$c(x, y; t = 0) = 0 \text{ for } 0 \leq x \leq 1, 0 \leq y < 1 \tag{23}$$

The x-axis and y-axis were divided into $N = 50$ intervals. The length of the interval was chosen at $L = 1$, making $\Delta x$ and $\Delta y$ equal to $L/N = 1/50$. $\Delta t = 2.5 \cdot 10^{-7}$ with $t_{max} = 0.1$. For a stable system, the constraint as shown in equation 15 must hold. In order to meet this condition, $D$ was set to 1.

### C. The Time Independent Diffusion Equation

For each of the three iteration methods analysed in this report, the same parameters were used for the system. The length each side of the square domain was $L = 1$. The axis of the domain were divided into $N = 1000$ intervals, such that $\Delta x = L/N$ in equation 7 becomes $\Delta x = 1/1000$. The $\epsilon$ as defined in the stopping condition in equation 15 is chosen at $\epsilon = 10^{-6}$.

In addition to the analysis of these methods on the system as described in the theory section, the Successive Over Relaxation method was also analysed by measuring how the iteration time depends on the number of objects that were suspended in the system. These objects were defined as cubes with a constant $c(i,j) = 0$ in the surface of the objects. The dimensions of the cubes were $6\delta x$ by $6\delta x$. One to four objects were included in the computational domain (figure 9).

## IV. Results

### A. One Dimensional Wave Equation

Figure 2 shows numerical solutions for the one dimensional wave equation at different time points. Figure 2a shows solutions for the initial condition $\Psi(x, t = 0) = \sin(2\pi x)$. Figure 2b shows solutions for the initial condition $\Psi(x, t = 0) = \sin(5\pi x)$ and figure 2c shows solutions for the initial condition $\Psi(x, t = 0) = \sin(5\pi x)$ (if $1/5 < x < 2/5$, else $\Psi = 0$). Animated plots of the time development of the solutions in figure 2 can be found in the zip file included with this report.

### B. Time Dependent Diffusion Equation

Figure 3 shows the numerical solutions of the time dependent wave equation at different time points. In this figure, we can see that the concentration spreads from the top side to the bottom side of the domain. The animated plot of figure 3 can be found in the included zip file.

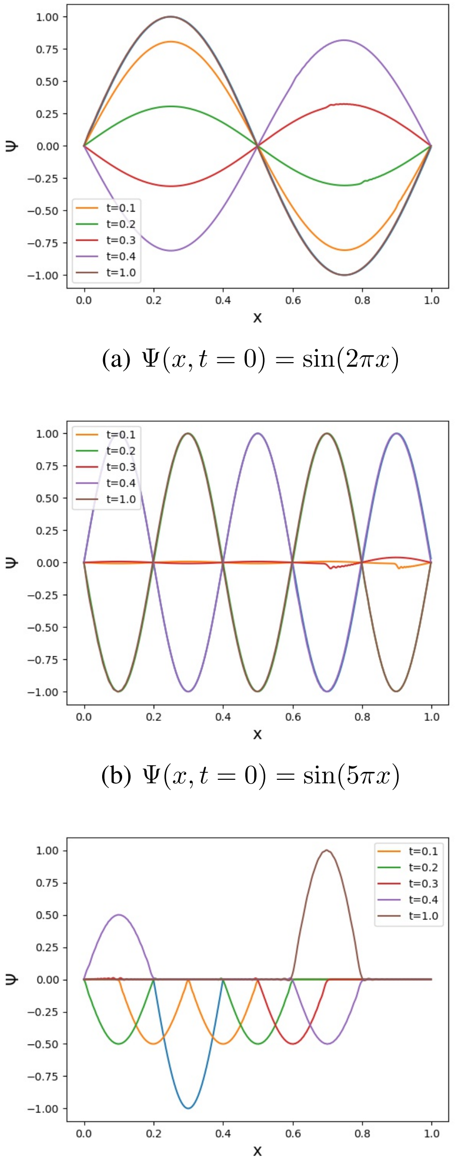

(a) $\Psi(x, t = 0) = \sin(2\pi x)$

(b) $\Psi(x, t = 0) = \sin(5\pi x)$

(c) $\Psi(x, t = 0) = \sin(5\pi x)$ (if $1/5 < x < 2/5$, else $\Psi = 0$)

Fig. 2: Numerical solutions of the one dimensional wave equation at different time points (t=0.1,t=0.2,t=0.3,t=0.4,t=1). a) The initial condition of the first system is $\Psi(x, t = 0) = \sin(2\pi x)$. b) The initial condition of the second system is $\Psi(x, t = 0) = \sin(5\pi x)$. c) The initial condition of the third system is $\Psi(x, t = 0) = \sin(5\pi x)$ (if $1/5 < x < 2/5$, else $\Psi = 0$).

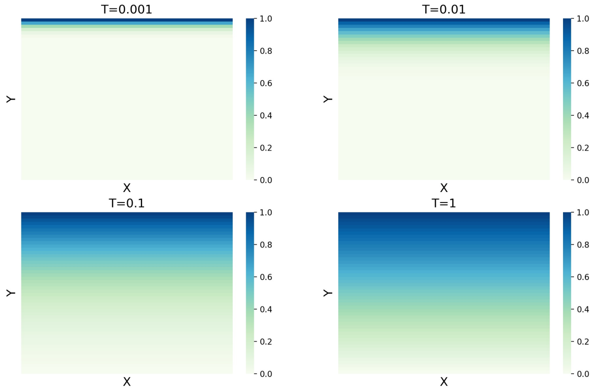

Fig. 3: Two dimensional time developments of the numerical time dependent diffusion equation model. The 4 plot show the concentrations at t = 0.001, t = 0.01, t = 0.1 and t = 1.

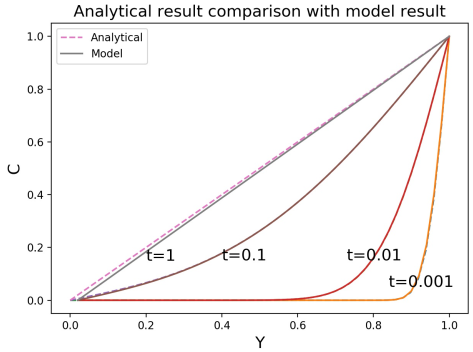

Fig. 4: Concentration as a function of $y$ at different time points (t = 1, t = 0.1, t = 0.01 and t = 0.001). The numerical solutions are represented by full lines and the analytical solutions are represented by dotted lines.

Figure 4 shows the concentration in a slice of the numerical system perpendicular to the x-axis as a function of $y$ ($c(y)$). This concentration is shown for the numerical solution at different time points (t = 0.001, t = 0.01, t = 0.1 and t = 1), as well as for the analytical solution at these time points. From this figure we can see that the numerical solution agrees with the analytical solution as described by equation 11. Only at t = 1, the numerical solution deviates visibly from the analytical solution.

### C. Time Independent Diffusion Equation

As discussed in the theory section of this report, there exist various iterative methods to solve the time independent diffusion equation. To test the correctness of these methods, the concentration in a slice of the

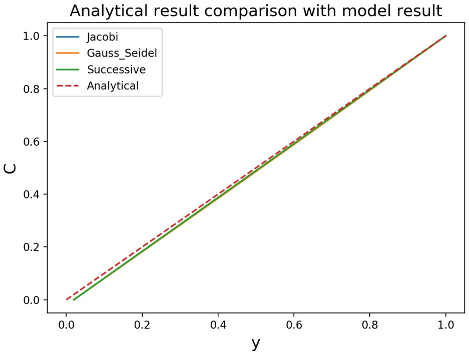

Fig. 5: Three time independent methods compared with the analytical solution. The red dashed line is the analytical solution and the lines of the three time independent methods are overlapping. $\delta = 10^{-6}$ for all methods. For the ROC method, $\omega = 1.8$.

systems perpendicular to the x-axis was compared to the analytical solution (figure 5). In figure 6 it is shown that the error of the numerical methods increases as the spatial coordinate $y$ moves from $y = 1$ to the middle of the y-axis, and then decreases again as it approaches $y = 0$. A possible explanation of this phenomenon can be found in the Discussion section.

To analyse the relation between the number of iterations and the convergence measure $\delta$ (as defined in equation 20), the various algorithms have been executed for different values of $\delta$. For each of these instances the iteration time has been measured. Figure 7 shows iteration times of the various methods against $p$, with $p = -log(\delta)$.

For the Successive Over Relaxation method, the influence on the number of x and y intervals on the optimal $\omega$ was analysed. Figure 7 shows how the $\omega$ influenced the iteration time.

Another test of the Successive Over Relaxation method was to analyse how the inclusion of objects in the computational domain influenced the number of iterations. Figure 10 shows this relation for a range of $\omega = 1.7$ to $\omega = 2$ for 0 to 4 objects.

## V. Discussion

### A. One Dimensional Wave Equation

As figure 2 and the included animations show, the wave equation will decay or increase at the different $x$ positions with change in time. From these figures we can also see that different initial conditions gave the wave equation different shapes and dynamics.

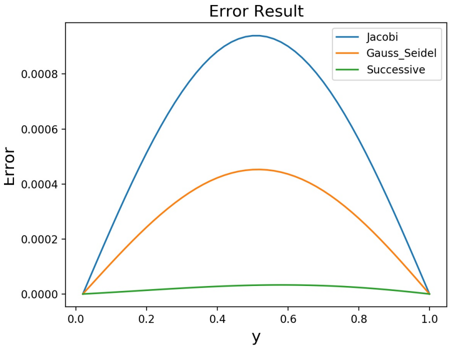

Fig. 6: Three time independent methods compared with the analytical solution. Absolute error was measured by the difference between analytical solution and results of three methods.

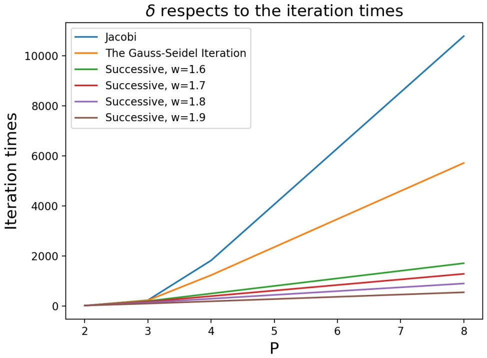

Fig. 7: $\delta$ with respect to the iteration times for three time independent methods.$p = -log(\delta)$

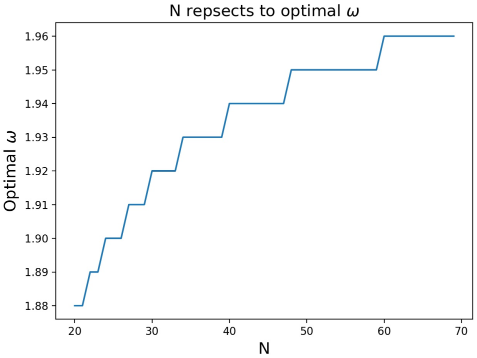

Fig. 8: The optimal value for $\omega$ changes with the number of intervals $N$, the range of $N$ is$(20, 70)$, and the step is 1.

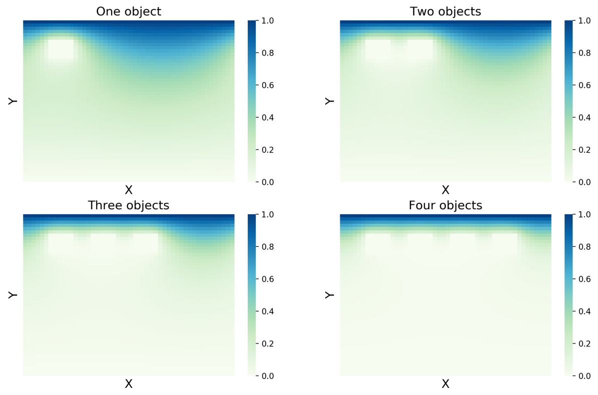

Fig. 9: Different number of objects in computational domain. The size of each cube is $6 * 6$.

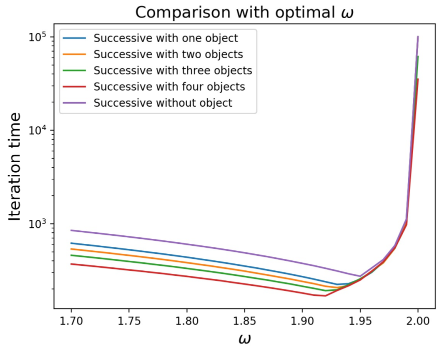

Fig. 10: Iteration time (number of iterations) vs. the optimal omega for the ROC method for different numbers of objects included in the domain.

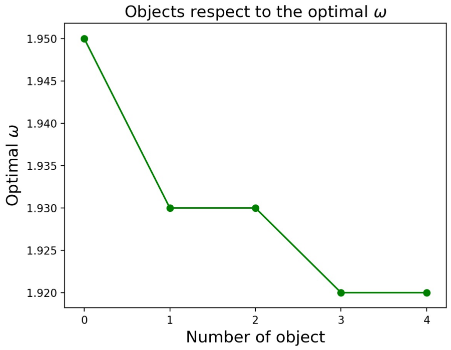

Fig. 11: The optimal value for $\omega$ versus the number of objects included in the domain for the ROC method.

### B. Time Dependent Diffusion Equation

As figure 3 shows, the concentration as computed by the numerical algorithm diffuses from the source to the sink over time. Across time, the concentration away from the source increases with a rate depending on the distance from the source. Figure 4 shows that as time increases, the concentration across space seems to approach a linear dependence on $y$. When comparing the numerical solutions to the analytical solutions at different time points (figure 4), it can be observed that the numerical solutions seem to agree with the analytical solutions. However, at $t = 1$ it is clear that there exists an error between the analytical solution and the result of the model. This could be explained by the fact that the analytical solution depends on an infinitely small $\delta t$. This suggests that as $\delta t$ approaches an infinitely small value for a theoretical numerical scheme, the solution would approach the linear dependence $c(y) = y$ at $t = 1$. Since $\delta t$ in the numerical scheme used is naturally larger than an infinitely small value, the numerical solution at $t = 1$ is not exactly equal to the analytical solution.

### C. Time Independent Diffusion Equation

Figure 5 shows the results of Jacobi iteration, the Gauss-Seidel method and SOR compared with the analytical results. The results of the three methods seem to be very similar, such that they are overlapping in the figure. However, when the results are compared to the analytical results, there is a visible error, just as with the results of the time dependent diffusion equation at $t = 1$ (figure 4). Figure 6 shows this error across $y$. The absolute error of three methods has an arched shape, and the Jacobi seems to have the largest error when compared to the other two methods, followed by the Gauss-Seidel method. The SOR method seems to have the smallest error. This suggests that the inclusion of currently calculated concentrations in the Gauss-Seidel method increases the accuracy of this method. Additionally, these results suggest that the inclusion of the $\omega$-term in the Gauss-Seidel method, as is done to create the SOR method, increases the accuracy of the method significantly. Figure 6 also shows that the error peaks at the middle of the $y$-range. A possible explanation for this could be the fact that the concentrations at $y = 0$ and $y = 1$ are fixed at $c = 0$ and $c = 1$ in the algorithm, and as such the error with the analytical solution is zero. The exact concentrations at $y = 0$ and $y = 1$ are then used as reference points in the iterations, which causes the error to increase the further away from these exact points the concentrations are calculated. With this reasoning, the $y$ value with the highest error will be the point with the largest distance from both $y = 0$ and $y = 1$, which is in the middle of the $y$-range.

Figure 7 shows how the stop condition $\delta$ influences the number of iterations. It is clear to see that the iteration time increases with decreasing $\delta$. When the stop condition $\delta$ is smaller than $10^{-3}$, the iteration times increase significantly, with Jacobi iteration as the most significant increase, followed by the Gauss-Seidel method and finally the SOR method. This suggests that the SOR method is not only the most accurate method, as discussed above, but also the fastest method. This figure also shows that $\omega$ influences the number of iterations of the SOR method. For the number of $x$ and $y$ intervals ($N = 50$) that was used in the method, it seemed that $\omega = 1.95$ was the optimal value (figure 11).

From figure 8, it can be observed that there is a general trend with which the the optimal value for $\omega$ increases when the number of spacial intervals increases. There seems to be a step like behaviour in this relation. Moreover, it seems that the slope in this increase in optimal $\omega$ decreases as the number of spacial intervals increases. A possible explanation for this could be that a more aggressive update method works better when the concentration needs to be calculated for to a larger amount of points in the domain.

Figure 10 and 11 show the influence of the inclusion of sink-like objects in the domain in the SOR method. Figure 10 shows that the number of iterations decreases when the number of objects increases. A possible explanation for this could be that the objects hinder the spread of the concentration in the domain. This causes the convergence rates to become comparatively faster when the number of objects increases. Figure 11 shows that the optimal $\omega$ decreases when the number of objects increases. This could possibly be explained by figure 8. Since an increase in number of objects decreases the points that need to agree with the stopping condition, it could be that this effectively decreases the number of intervals. From figure 8 we can see that a decrease in number of intervals decreases the optimal $\omega$.

It could be interesting to investigate the behaviour of the numerical solution when adding an insulating material to the domain. As a suggestion for further research, a possible way to implement this is by making the boundary concentrations of the insulating material equal to the concentration of the spatial point that is being calculated. For the Jacobi iteration, this would mean that the concentration of a point at the left side of such an object would be calculated by equation 24. This equation is different from equation 19 by the fact that $c^k_{i-1,j}$ is replaced by $c^k_{i,j}$.

$$c^{k+1}_{i,j} = \frac{1}{4}\left(c^k_{i,j} + c^k_{i-1,j} + c^k_{i,j+1} + c^k_{i,j-1}\right) \tag{24}$$

## VI. Conclusion

In this report, the one dimensional wave equation and the two dimensional diffusion wave equation has been discussed and analysed. For the wave equation, the stepping method has been use to discretize the wave equation. The results of different initial condition and boundary conditions seem to have different shapes and dynamics.

For the two dimensional time dependent diffusion equations, for the given initial condition and periodic boundary conditions, the concentration diffuses from the source to the sink with the changing time and when $t = 1$, the system reaches equilibrium. However, the results from the model still have an error when compared to the analytical solution. This could be caused by the fact that the time step $\delta t$ is not infinitely small in the model.

For the two dimensional time independent diffusion equations, the Jacobi method has the slowest convergence rate and SOR has the fastest convergence rate in any stop condition $\delta$. When compared to the analytical solution, Jacobi has the largest error and SOR has the smallest error. For the SOR method, a greater number of $x$ and $y$ intervals increases the optimal $\omega$ because large intervals increase the number of iteration and delay the threshold point (optimal $\omega$). Additionally, objects are included into the model. Increasing number of objects decreases the number of iterations. This could be explained by the fact that the objects hinder the concentration from spreading to the sink and stop at $\delta$ early. Additionally, the optimal $\omega$ also decreases when the number of objects increases.

## References

[1] Michael T. Heath. *Scientific Computing: An Introductory Survey*, volume 24. 2007.

[2] Rudolf Gorenflo, Francesco Mainardi, Marco Raberto, and Enrico Scalas. Fractional diffusion in finance: Basic theory. In *A Review Paper Based on a Talk Given by F. Mainardi at MDEF2000-Workshop 'Modelli Dinamici in Economia e Finanza', Urbino (Italy)*, 2000.